

Josephson threshold detector in the phase diffusion regime

Dmitry A. Ladeynov,^{1,2,3} Andrey L. Pankratov,^{1,2,3} Leonid S. Revin,^{1,3} Anna V. Gordeeva,^{1,3} and Evgeny V. Il'ichev⁴

¹*Nizhny Novgorod State Technical University n. a. R. E. Alekseev, Nizhny Novgorod, Russia*

²*N. I. Lobachevsky State University of Nizhny Novgorod, Nizhny Novgorod, Russia*

³*Institute for Physics of Microstructures of RAS, Nizhny Novgorod, Russia*

⁴*Leibniz Institute of Photonic Technology, Jena, Germany*

We demonstrate that the performance of threshold detectors based on Al Josephson junctions can be significantly improved by exploiting the phase diffusion regime. When the escape dynamics of the detector switches to this regime, a decrease in both - dark count rate and the standard deviation of switching current is simultaneously observed. However, this effect is essential for (i) critical currents below 100 nA, and (ii) temperatures of the order of several hundreds millikelvin. Importantly that for such detectors optimal performance occurs at finite temperatures, making the microwave single photon detection feasible even in the sub-K range. Possible explanation of these findings is discussed.

Modern developments in quantum communications and quantum information processing devices benefit greatly from the efficient detection of individual photons. However, widely used conventional single-photon detectors, such as superconducting nanowires [1–3] or transition-edge devices [4, 5], require a sufficiently high incident photon energy to modify the state of the detector. For the microwave frequency range, the corresponding energy is rather low, about 10 yJ. Consequently, efficient single photon detectors for microwave field have not been implemented yet. A natural idea for realizing such a detector is to exploit quantum Josephson circuits. Indeed, superconducting qubits, being two-level quantum systems with characteristic energy in the microwave scale, can be excited by absorbing an incident photon. Various types of qubit-based photon detectors have been proposed and implemented [6–15].

One of the possible technical solutions here is to use a basic variant of the phase qubit [16] which is a current-biased Josephson junction (CJJ). The phase across the junction for such devices is associated with the dynamics of a quantum particle in a washboard potential [17], see Figure 1 (a). In the initial state of the detector, the particle is trapped in one of the local potential minima and the voltage across the CBJJ is zero. After the incident microwave field delocalizes the trapped particle, it escapes to the “running state” (RS), providing a finite voltage across the CBJJ. This voltage is in the millivolt range and can be easily measured.

However, to realize maximum sensitivity, the CBJJ must be biased relatively close to the critical current value. Due to fluctuations, such initialization causes uncontrolled transitions to a voltage state, corresponding to the dark count rate. The trade-off between initialization point and resolution, which is common for threshold-type detectors, is clearly seen for this particular realization. In fact, this is the main obstacle to implementing an efficient single photon detector for the microwave range. Importantly, that relatively long lifetime of the threshold

detector in the initial (zero-voltage) state is a key issue for Dark Matter axion-type particle searches [18–24].

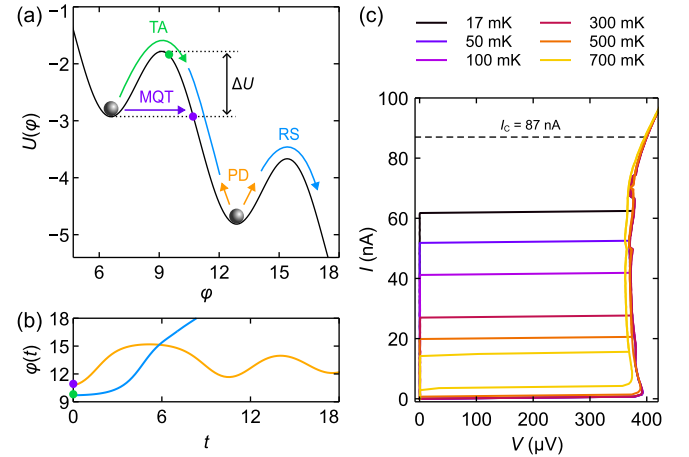


Figure 1. (a) Phase particle regimes in a tilted potential. Here, TA means thermal activation, MQT - macroscopic quantum tunneling, RS - switching to the running state with finite voltage and PD - phase diffusion regime with re-trapping. (b) Phase evolution. If a particle escapes due to TA, it gains larger potential energy (green dot), and thus has a higher probability of switching to RS. If a particle tunnels under the barrier (violet dot), it has smaller potential energy and higher probability of re-trapping, leading to quantum PD. (c) IVC of SIS2; dashed line is theoretical critical current.

Various approaches have been used to optimize the CBJJ threshold detector [25–36]. The experimentally demonstrated resolution of 5 photons with marginal single photon detection in the clicking regime at 10 GHz appears to be the best to date [37]. Interestingly, that the theoretically estimated lifetime in the zero voltage state for the studied threshold detector is sufficiently shorter than the experimental one. To explain this inconsistency, it has been proposed that CBJJ is in the so-called phase diffusion regime [37].

The main feature of the phase diffusion (PD) regime,

in a handwaving manner, can be commented on as follows. After the escape from the local minimum of the washboard potential via macroscopic quantum tunneling (MQT) or thermal activation (TA), the phase can be re-trapped into another minimum with a relatively high probability, see Figure 1 (a,b). Consequently, in the PD regime the CBJJ much rarely switches to the voltage state due to re-trapping, which effectively increases its lifetime in the initial state. However, in the case of arriving photon, switching into the running state without re-trapping may occur, due to the induced current pulse that significantly exceeds the detector threshold. In spite of the fact that characteristics of the phase diffusion regime are well described [37–51], switching dynamics between zero and voltage states still requires additional study. In this paper, we demonstrate that by exploiting this regime, an efficient microwave single photon detector can be realized.

Intuitively, a sensitive CBJJ detector should exhibit a relatively low critical current (below we prove this statement, see Figure 4). By making use of a self-aligned shadow evaporation technique [37, 51, 52], several superconductor-insulator-superconductor (SIS) Al/AlO_x/Al tunnel junctions of various areas from several squared microns to sub-micron size with the critical current below 1 μ A were fabricated. The analysis of experimental data was carried out based on measurements of 3 different CBJJs: SIS1 with dimensions $14 \times 0.5 \mu\text{m}^2$, SIS2 – $2 \times 0.4 \mu\text{m}^2$ and SIS3 – $2 \times 1 \mu\text{m}^2$. The samples were thermally anchored to the mixing chamber plate of a dry dilution refrigerator, providing a minimum nominal temperature of about 12 mK, and surrounded by both mu-metal and superconducting shields, also decreasing background radiation [53]. To minimize low frequency noise, the anti-vibration dampers for the fridge body were used. The switching current distributions $W(I)$ were reconstructed by measuring the switching statistics of a CBJJ from a zero-voltage state to a finite voltage state in the temperature range between 15 mK and 1 K. To perform these measurements, a bias current applied to the junction was ramped up at a constant rate I_v with 5000 repetitions. Here, well-filtered twisted-pair lines were used for conventional four-point measurements.

An example of the current-voltage characteristic (IVC) for the SIS2 sample is shown in Figure 1 (c). Here the theoretical critical current (87 nA, dashed line) was restored using the CBJJ parameters. Similarly, critical currents for the SIS1 and SIS3 were obtained equal to 895 nA and 270 nA, respectively. From the measurements of the switching current distributions we extract the mean switching current $\langle I_{\text{sw}} \rangle$ as well as the standard deviation σ at different temperatures. Results are presented in Figure 2.

Qualitatively, the temperature dependence of the standard deviation is similar for all samples, see Figure 2 (a), and three main switching regimes of the CBJJ are clearly

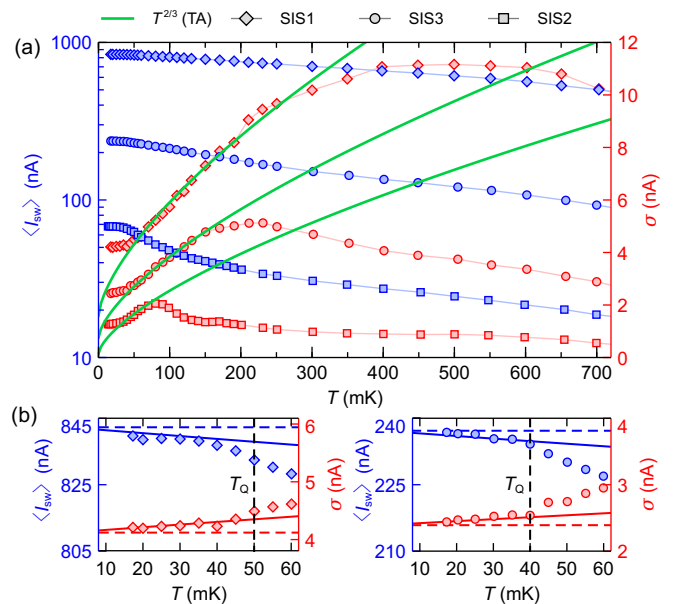


Figure 2. (a) The blue markers are the mean switching current $\langle I_{\text{sw}} \rangle$ and the red markers are the standard deviation σ . Green solid curves show the TA mechanism $\sigma \sim T^{2/3}$ [54]. (b) Experimental data set of the mean switching current and standard deviation in comparison with the MQT theory (dashed curves) and MQT theory with substitution of $\hbar\omega_0 + k_B T$ instead of $\hbar\omega_0$ (solid curves) for SIS1 and SIS3.

visible here. At low temperatures MQT determines the dynamics of the detector. Indeed, below 50 mK the $\sigma(T)$ dependence is saturated, see Figure 2 (a). However, unlike MQT theory which predicts $\sigma(T) = \text{const}$, detailed measurements demonstrate a finite slope of this dependence, see Figure 2 (b). Presumably, the switchings here are caused not only by MQT events, but also accompanied by TA transitions. Indeed, these results can be well-fitted by the standard formulas of the MQT theory [55, 56], substituting $\hbar\omega_0 + k_B T$ instead of $\hbar\omega_0$:

$$\tau_Q = \frac{2\pi}{\omega_0} \sqrt{\frac{2\pi}{B}} e^B, \quad B = \frac{\Delta U[7.2 + 8A/Q]}{\hbar\omega_0 + k_B T},$$

where $\Delta U(i) = 2E_J [\sqrt{1-i^2} - i \arccos i]$ with $i = I/I_C$ and Josephson energy $E_J = \hbar I_C/2e$. The plasma frequency and the junction quality factor are expressed as $\omega_0 = \sqrt{2eI_C/\hbar C} (1-i^2)^{1/4}$ and $Q = \omega_0 R_N C$. Here \hbar is the Planck constant and e is the electron charge, R_N is the normal Josephson junction resistance and C is its capacitance, $A \sim 10$ is numerical fitting parameter.

As temperature increases, the growth of $\sigma(T)$ accelerates. This indicates the transition between MQT regime (with small number of TA events) and dominating TA dynamics. Here the dependence $\sigma(T)$ can be approximated by the function $T^{2/3}$ (see green curves in Figure 2 (a)), known for TA switching [54]. Consequently, a separation between MQT and TA regimes (quantum crossover) is

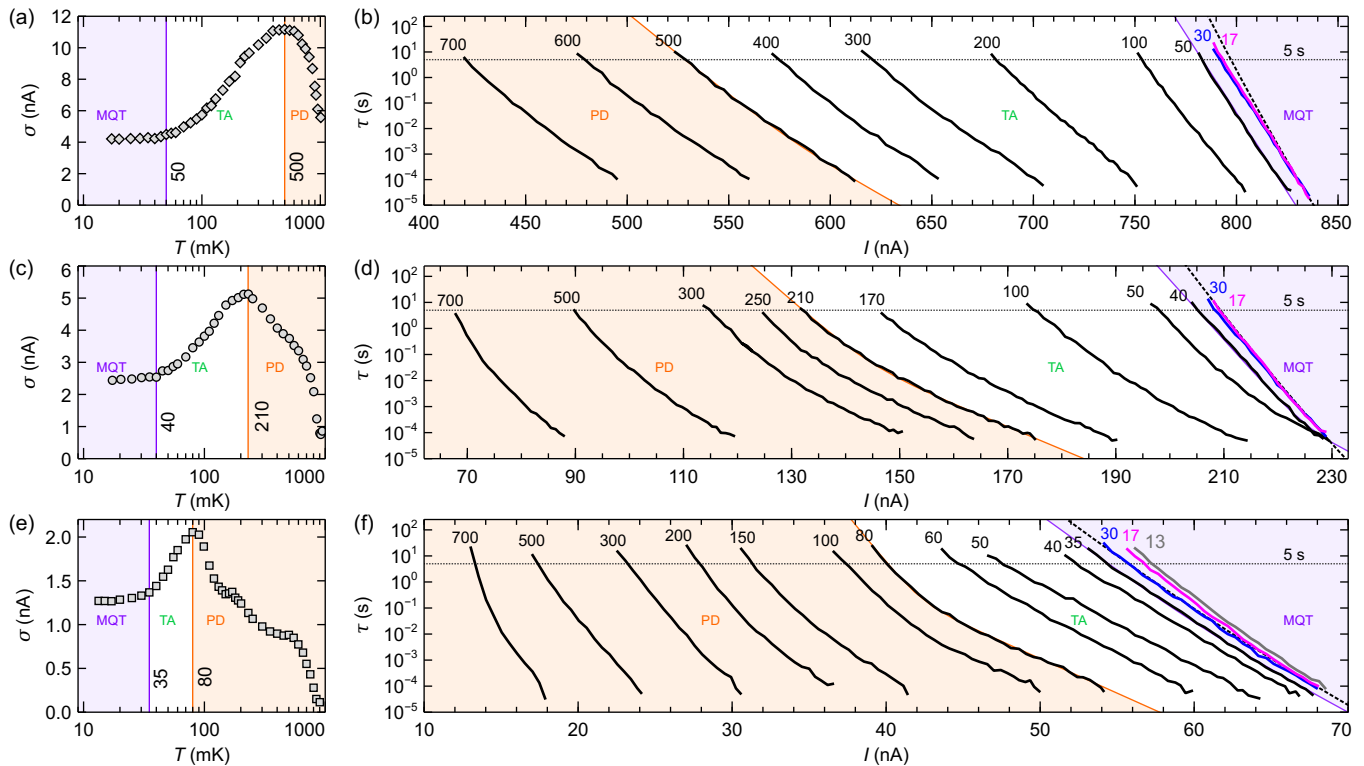


Figure 3. Standard deviation of switching currents (left) and lifetimes (right) for different sample temperatures. (a, b) SIS1; (c, d) SIS3; (e, f) SIS2. The violet area corresponds to MQT regime, the white area corresponds to TA regime, the orange area corresponds to the PD regime. Each lifetime curve is marked by its temperature in mK. Dashed line is the MQT theory lifetime.

clearly visible. With further temperature increase, a deviation from TA behavior due to transition to the phase diffusion regime is observed.

In spite of different nominal critical currents (87 nA, 270 nA and 895 nA) all these CBJJs demonstrate the transition to the phase diffusion regime (the point of deviation of $\sigma(T)$ from $T^{2/3}$ dependence, see Figure 2 (a)).

In addition to switching current distributions, an important characteristic for microwave single photon detector applications is the lifetime of zero voltage state (dark count time) $\tau(T)$. In Figure 3 (b,d,f) the dark count time curves $\tau(T)$ as a function of bias current and temperature (shown in mK at each curve) are presented. Here, the important characteristic of the lifetime is not only its value at a certain bias current, but also its tilt. It is obvious, that for more steeper tilts, taking the desired dark count time value, one can more closely approach the critical current, thus decreasing the detection threshold and improving the sensitivity. Usually, it is assumed that the lifetime tilt increases with decreasing temperature, which is not always so, as we show below.

By making use of experimental data of $\sigma(T)$ (Figure 3 (a,c,e)) we present different switching regimes for lifetimes $\tau(T)$ (Figure 3 (b,d,f)). Areas of different types of switching are highlighted: MQT (violet area), TA (white area), PD (orange area). Essentially, that all samples behave

similarly and differ in the scale of each region only. A tendency here is visible in Figure 3: the lower the critical current of the sample, the more narrow the white region TA and the broader the orange region PD, and the MQT area is reduced as well.

Usually, below the quantum crossover temperature, the lifetime can be predicted by the MQT theory [35, 55, 56], but for the quantum phase diffusion regime some corrections are expected. Basically, quantum PD can manifest itself as an increase in lifetimes compared to those calculated by MQT theory. However, for CBJJs with high critical current the quantum PD effect was not demonstrated. Indeed for SIS1 ($I_C = 895$ nA) the experimentally observed lifetime is even shorter than predicted by theory, see Figure 3 (b), curve at 17 mK. For SIS3 sample ($I_C = 270$ nA) the theoretical expectation is consistent with experimental observation, see Figure 3 (d), curve at 17 mK. Visible improvement of the lifetime is observed for SIS2 only ($I_C = 87$ nA), see Figure 3 (f), curve at 13 mK. In spite of the fact that quantum PD regime is observed here, it does not seriously improve the detector performance. For instance, for the same lifetime of 5 s the difference between the predicted by MQT bias current and experimental one is 1 nA only. This is not sufficient since the photon-induced current pulse itself is of about 20 nA, see below.

In the TA regime lifetimes, like the standard deviation, are traditionally described by the theory based on the Kramers expression $\tau(T) \sim \exp \Delta U/k_B T$ [57]. However, this description does not apply to the PD regime. Indeed, $\sigma(T)$ decreases with increasing temperature, reaching values even below the quantum saturation level at low temperatures, see Figure 3 (c,e). In parallel, the lifetime tilt $|d\tau/dI|$ increases as well, indicating that larger bias current can be used for the same lifetime τ .

Since we have determined the mean switching currents and lifetimes as a function of temperature and bias current for our CBJJs, we can analyse their performance as single photon detectors. Assuming an ideal coupling between the CBJJ and the incident photons, following [29], the photon-induced current can be estimated with account of the CBJJ losses, described by the quality factor $Q = \omega_0 R_N C$. In this case the photon energy $\hbar\omega_{\text{ph}}$ transfers to the energy of the SIS current, therefore $I_{\text{ph}} = \sqrt{2\hbar\omega_{\text{ph}}L_J^{-1}(1+2\pi/Q)^{-1}}$, where $L_J = \hbar/(2e\sqrt{I_C^2 - I^2})$ is the Josephson inductance.

As it follows from the expression above, the photon-induced current pulse amplitude differs for investigated CBJJs since they have different parameters. Indeed, for SIS1 sample, at frequency 10 GHz, the magnitude of the current pulse is about 50 nA with a weak temperature variation. For samples with smaller critical currents the magnitude of the current pulse depends on temperature. For SIS3 this magnitude changes from 25 nA to 35 nA, for SIS2 from 12 nA to 22 nA when temperature drops from 700 mK to 17 mK.

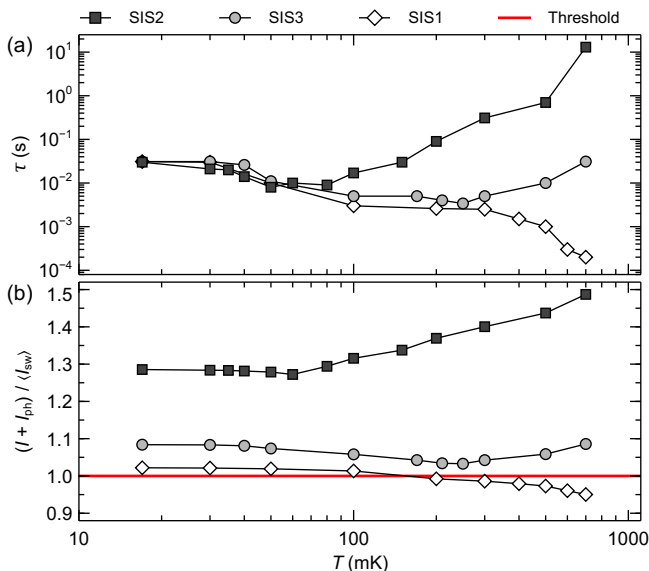


Figure 4. (a) Lifetime with a fixed shift in bias current ($I = \langle I_{\text{sw}} \rangle - \Delta I$) for each sample: SIS1 - $\Delta I = 25$ nA, SIS3 - $\Delta I = 18$ nA and SIS2 - $\Delta I = 6$ nA. (b) Normalized total current $(I + I_{\text{ph}}) / \langle I_{\text{sw}} \rangle$ due to absorption of the 10 GHz photon versus temperature of samples. The threshold is a normalized critical current.

To demonstrate temperature dependences of lifetimes, we fixed a bias current shift $\Delta I = \langle I_{\text{sw}} \rangle - I$, taking it to be sufficiently smaller than the magnitude of the photon-induced current pulse to ensure proper switching of the detector. For each sample, we take the following values: SIS1 - $\Delta I = 25$ nA, SIS3 - $\Delta I = 18$ nA and SIS2 - $\Delta I = 6$ nA. The corresponding lifetime values, subtracted from Figure 3 (b,d,f), are presented in Figure 4 (a).

Additionally, by choosing the desired dark count time, $\tau = 5$ s, as shown in Figure 3 (b, d, f) by dotted line, we can reconstruct the corresponding bias current values for each temperature. Selecting as an example the photon frequency of about 10 GHz [24], and taking into account $I_C(T)$ dependence, we calculated the induced currents. Unambiguous switching of the detector occurs if $I + I_{\text{ph}} > \langle I_{\text{sw}} \rangle$. Results of our estimates are summarized in Figure 4 (b). The switching threshold is indicated in this figure by the red line.

The switching characteristics of CBJJ between zero and finite voltage states in the phase diffusion regime, presented in Figure 4, are quite unusual. While for the sample with higher critical current (SIS1, $I_C = 895$ nA) both lifetime and total switching current $(I + I_{\text{ph}}) / \langle I_{\text{sw}} \rangle$ decrease with temperature rise as expected, samples with lower critical currents exhibit non-monotonic behaviour. A decrease of the lifetime and the total switching current at temperatures slightly above a crossover temperature between the MQT and TA regimes is "compensated" by an increase of these values in the PD regime. Importantly, that for samples with lower critical current this increase is more pronounced. This observation is counter-intuitive. Indeed, as the critical current I_C decreases, the well depth of the washboard potential becomes smaller, since $E_J \sim I_C$, see Figure 1 (a). Automatically the ratio between the Josephson E_J and the thermal energies $k_B T$ decreases. Consequently, the transition to the running (finite voltage) state requires less thermal energy, which contradicts the experiment. Qualitatively it can be explained as follows. With increase of the temperature the probability of escaping particle re-trapping in an adjacent potential well increases. Since the threshold detector recognizes the only difference between zero and finite voltage states, it ignores noise-induced escapes, unless these escapes produce finite voltage, which improves overall detector performance. Theoretical explanation of this effect requires further study with outlining the roles of damping and temperature on the CBJJ dynamics.

Conclusions We have experimentally demonstrated that the performance of a threshold detector, based on switching dynamics of Al-made Josephson junctions with relatively small critical currents, can be essentially improved by increasing working temperature. Thus, single photon detection at 10 GHz can be approached even at sub-K temperatures. This contradictory observation is explained by the transition of the switching dynamics to the phase diffusion regime. Moreover, the standard devi-

ation of switching current in this regime is smaller than that observed at the lowest temperatures, where switching is determined primarily by the macroscopic quantum tunneling. In addition, in the quantum tunneling regime, we observe a finite slope of the quantum saturation level due to finite operating temperatures.

The work is supported by the Russian Science Foundation (Project 19-79-10170).

-
- [1] I. Esmail Zadeh, J. Chang, J. W. N. Los, S. Gyger, A. W. Elshaari, S. Steinhauer, S. N. Dorenbos, and V. Zwiller, *Applied Physics Letters* **118**, 10.1063/5.0045990 (2021).
- [2] S. Khasminskaya, F. Pyatkov, K. Slowik, S. Ferrari, O. Kahl, V. Kovalyuk, P. Rath, A. Vetter, F. Hennrich, M. M. Kappes, G. Gol'tsman, A. Korneev, C. Rockstuhl, R. Krupke, and W. H. P. Pernice, *Nature Photonics* **10**, 727 (2016).
- [3] O. Kahl, S. Ferrari, V. Kovalyuk, G. N. Goltsman, A. Korneev, and W. H. P. Pernice, *Sci. Rep.* **5**, 10941 (2015).
- [4] K. D. Irwin and G. C. Hilton, *Transition-Edge Sensors*, in *Cryogenic Particle Detection* (Springer, Berlin, Heidelberg, Germany, 2005) pp. 63–150.
- [5] M. Förtsch, T. Gerrits, M. J. Stevens, D. Strekalov, G. Schunk, J. U. Fürst, U. Vogl, F. Sedlmeir, H. G. L. Schwefel, G. Leuchs, S. W. Nam, and C. Marquardt, *J. Opt.* **17**, 065501 (2015).
- [6] B. R. Johnson, M. D. Reed, A. A. Houck, D. I. Schuster, L. S. Bishop, E. Ginossar, J. M. Gambetta, L. DiCarlo, L. Frunzio, S. M. Girvin, and R. J. Schoelkopf, *Nature Physics* **6**, 663 (2010).
- [7] K. Inomata, Z. Lin, K. Koshino, W. D. Oliver, J.-S. Tsai, T. Yamamoto, and Y. Nakamura, *Nature Communications* **7**, 1 (2016).
- [8] J.-C. Besse, S. Gasparinetti, M. C. Collodo, T. Walter, P. Kurpiers, M. Pechal, C. Eichler, and A. Wallraff, *Phys. Rev. X* **8**, 021003 (2018).
- [9] B. Royer, A. L. Grimsmo, A. Choquette-Poitevin, and A. Blais, *Phys. Rev. Lett.* **120**, 203602 (2018).
- [10] S. Kono, K. Koshino, Y. Tabuchi, A. Noguchi, and Y. Nakamura, *Nature Physics* **14**, 546 (2018).
- [11] R. Lescanne, S. Deléglise, E. Albertinale, U. Réglade, T. Capelle, E. Ivanov, T. Jacqmin, Z. Leghtas, and E. Flurin, *Phys. Rev. X* **10**, 021038 (2020).
- [12] E. Albertinale, L. Balembois, E. Billaud, V. Ranjan, D. Flanigan, T. Schenkel, D. Estève, D. Vion, P. Bertet, and E. Flurin, *Nature* **600**, 434 (2021).
- [13] A. L. Grimsmo, B. Royer, J. M. Kreikebaum, Y. Ye, K. O'Brien, I. Siddiqi, and A. Blais, *Phys. Rev. Appl.* **15**, 034074 (2021).
- [14] A. V. Dixit, S. Chakram, K. He, A. Agrawal, R. K. Naik, D. I. Schuster, and A. Chou, *Phys. Rev. Lett.* **126**, 141302 (2021).
- [15] L. Balembois, J. Travesedo, L. Pallegoix, A. May, E. Billaud, M. Villiers, D. Estève, D. Vion, P. Bertet, and E. Flurin, *Phys. Rev. Appl.* **21**, 014043 (2024).
- [16] J. M. Martinis, S. Nam, J. Aumentado, and C. Urbina, *Phys. Rev. Lett.* **89**, 117901 (2002).
- [17] A. Barone and G. Paternò, *Physics and applications of Josephson effect* (John Wiley & Sons, New York, 1982).
- [18] P. Sikivie, *Rev. Mod. Phys.* **93**, 015004 (2021).
- [19] I. G. Irastorza and J. Redondo, *Progress in Particle and Nuclear Physics* **102**, 89 (2018).
- [20] T. Braine, R. Cervantes, N. Crisosto, N. Du, S. Kimes, L. J. Rosenberg, G. Rybka, J. Yang, D. Bowering, A. S. Chou, R. Khatiwada, A. Sonnenschein, W. Wester, G. Carosi, N. Woollett, L. D. Duffy, R. Bradley, C. Boutan, M. Jones, B. H. LaRoque, N. S. Oblath, M. S. Taubman, J. Clarke, A. Dove, A. Eddins, S. R. O'Kelley, S. Nawaz, I. Siddiqi, N. Stevenson, A. Agrawal, A. V. Dixit, J. R. Gleason, S. Jois, P. Sikivie, J. A. Solomon, N. S. Sullivan, D. B. Tanner, E. Lentz, E. J. Daw, J. H. Buckley, P. M. Harrington, E. A. Henriksen, and K. W. Murch (ADMX Collaboration), *Phys. Rev. Lett.* **124**, 101303 (2020).
- [21] N. Crescini, D. Alesini, C. Braggio, G. Carugno, D. D'Agostino, D. Di Gioacchino, P. Falferi, U. Gambardella, C. Gatti, G. Iannone, C. Ligi, A. Lombardi, A. Ortolan, R. Pengo, G. Ruoso, and L. Taffarello, *Phys. Rev. Lett.* **124**, 171801 (2020).
- [22] O. Kwon, D. Lee, W. Chung, D. Ahn, H. Byun, F. Caspers, H. Choi, J. Choi, Y. Chong, H. Jeong, J. Jeong, J. E. Kim, J. Kim, Å. Kutlu, J. Lee, M. Lee, S. Lee, A. Matlashov, S. Oh, S. Park, S. Uchaikin, S. Youn, and Y. K. Semertzidis, *Phys. Rev. Lett.* **126**, 191802 (2021).
- [23] C. M. Adair, K. Altenmüller, V. Anastassopoulos, S. Arguedas Cuendis, J. Baier, K. Barth, A. Belov, D. Bozicevic, H. Bräuning, G. Cantatore, F. Caspers, J. F. Castel, S. A. Çetin, W. Chung, H. Choi, J. Choi, T. Dafni, M. Davenport, A. Dermenev, K. Desch, B. Döbrich, H. Fischer, W. Funk, J. Galan, A. Gardikiotis, S. Gninenko, J. Golm, M. D. Hasinoff, D. H. H. Hoffmann, D. Díez Ibáñez, I. G. Irastorza, K. Jakovčić, J. Kaminski, M. Karuza, C. Krieger, Ç. Kutlu, B. Lakić, J. M. Laurent, J. Lee, S. Lee, G. Luzón, C. Malbrunot, C. Margalejo, M. Maroudas, L. Miceli, H. Mirallas, L. Obis, A. Özbey, K. Özbozduman, M. J. Pivovarov, M. Rosu, J. Ruz, E. Ruiz-Chóliz, S. Schmidt, M. Schumann, Y. K. Semertzidis, S. K. Solanki, L. Stewart, I. Tsagris, T. Vafeiadis, J. K. Vogel, M. Vretenar, S. Youn, and K. Zioutas, *Nature Communications* **13**, 6180 (2022).
- [24] E. Graham, S. Ghosh, Y. Zhu, X. Bai, S. B. Cahn, E. Durcan, M. J. Jewell, D. H. Speller, S. M. Zacarias, L. T. Zhou, and R. H. Maruyama, *Phys. Rev. D* **109**, 032009 (2024).
- [25] Y.-F. Chen, D. Hover, S. Sendelbach, L. Maurer, S. T. Merkel, E. J. Pritchett, F. K. Wilhelm, and R. McDermott, *Phys. Rev. Lett.* **107**, 217401 (2011).
- [26] B. Peropadre, G. Romero, G. Johansson, C. M. Wilson, E. Solano, and J. J. García-Ripoll, *Phys. Rev. A* **84**, 063834 (2011).
- [27] P. Adesso, G. Filatrella, and V. Pierro, *Physical Review E* **85**, 016708 (2012).
- [28] A. Poudel, R. McDermott, and M. G. Vavilov, *Phys. Rev. B* **86**, 174506 (2012).
- [29] L. S. Kuzmin, A. S. Sobolev, C. Gatti, D. Di Gioacchino, N. Crescini, A. Gordeeva, and E. Il'ichev, *IEEE Trans. Appl. Supercond.* **28**, 2400505 (2018).
- [30] C. Guarcello, D. Valenti, B. Spagnolo, V. Pierro, and G. Filatrella, *Physical Review Applied* **11**, 044078 (2019).
- [31] C. Guarcello, A. Braggio, P. Solinas, G. P. Pepe, and F. Giazotto, *Physical Review Applied* **11**, 054074 (2019).

- [32] A. A. Yablokov, V. M. Mylnikov, A. L. Pankratov, E. V. Pankratova, and A. V. Gordeeva, *Chaos, Solitons & Fractals* **136**, 109817 (2020).
- [33] A. S. Piedjou Komnang, C. Guarcello, C. Barone, C. Gatti, S. Pagano, V. Pierro, A. Rettaroli, and G. Filatella, *Chaos, Solitons & Fractals* **142**, 110496 (2021).
- [34] A. A. Yablokov, E. I. Glushkov, A. L. Pankratov, A. V. Gordeeva, L. S. Kuzmin, and E. V. Il'ichev, *Chaos, Solitons & Fractals* **148**, 111058 (2021).
- [35] D. S. Golubev, E. V. Il'ichev, and L. S. Kuzmin, *Phys. Rev. Appl.* **16**, 014025 (2021).
- [36] D. A. Ladeynov, D. G. Egorov, and A. L. Pankratov, *Chaos, Solitons & Fractals* **171**, 113506 (2023).
- [37] A. L. Pankratov, L. S. Revin, A. V. Gordeeva, A. A. Yablokov, L. S. Kuzmin, and E. V. Il'ichev, *npj Quantum Information* **8**, 1 (2022).
- [38] J. M. Martinis and R. L. Kautz, *Phys. Rev. Lett.* **63**, 1507 (1989).
- [39] R. L. Kautz and J. M. Martinis, *Phys. Rev. B* **42**, 9903 (1990).
- [40] Y. Koval, M. V. Fistul, and A. V. Ustinov, *Phys. Rev. Lett.* **93**, 087004 (2004).
- [41] J. M. Kivioja, T. E. Nieminen, J. Claudon, O. Buisson, F. W. J. Hekking, and J. P. Pekola, *Phys. Rev. Lett.* **94**, 247002 (2005).
- [42] J. Männik, S. Li, W. Qiu, W. Chen, V. Patel, S. Han, and J. E. Lukens, *Phys. Rev. B* **71**, 220509 (2005).
- [43] V. M. Krasnov, T. Bauch, S. Intiso, E. Hürfeld, T. Akazaki, H. Takayanagi, and P. Delsing, *Phys. Rev. Lett.* **95**, 157002 (2005).
- [44] V. M. Krasnov, T. Golod, T. Bauch, and P. Delsing, *Phys. Rev. B* **76**, 224517 (2007).
- [45] J. C. Fenton and P. A. Warburton, *Phys. Rev. B* **78**, 054526 (2008).
- [46] Y. Yoon, S. Gasparinetti, M. Möttönen, and J. P. Pekola, *J. Low Temp. Phys.* **163**, 164 (2011).
- [47] H. F. Yu, X. B. Zhu, Z. H. Peng, Y. Tian, D. J. Cui, G. H. Chen, D. N. Zheng, X. N. Jing, L. Lu, S. P. Zhao, and S. Han, *Phys. Rev. Lett.* **107**, 067004 (2011).
- [48] L. Longobardi, D. Massarotti, G. Rotoli, D. Stornaiuolo, G. Papari, A. Kawakami, G. P. Pepe, A. Barone, and F. Tafuri, *Phys. Rev. B* **84**, 184504 (2011).
- [49] L. Longobardi, D. Massarotti, D. Stornaiuolo, L. Galletti, G. Rotoli, F. Lombardi, and F. Tafuri, *Phys. Rev. Lett.* **109**, 050601 (2012).
- [50] H. F. Yu, X. B. Zhu, H. Deng, G. M. Xue, Y. Tian, Y. F. Ren, G. H. Chen, D. N. Zheng, X. N. Jing, L. Lu, S. P. Zhao, and S. Han, *J. Phys. Conf. Ser.* **400**, 042079 (2012).
- [51] L. S. Revin, A. L. Pankratov, A. V. Gordeeva, A. A. Yablokov, I. V. Rakut, V. O. Zbrozhek, and L. S. Kuzmin, *Beilstein Journal of Nanotechnology* **11**, 960 (2020).
- [52] A. L. Pankratov, A. V. Gordeeva, L. S. Revin, D. A. Ladeynov, A. A. Yablokov, and L. S. Kuzmin, *Beilstein J. Nanotechnol.* **13**, 582 (2022).
- [53] R. Barends, J. Wenner, M. Lenander, Y. Chen, R. C. Bialczak, J. Kelly, E. Lucero, P. O'Malley, M. Mariantoni, D. Sank, H. Wang, T. C. White, Y. Yin, J. Zhao, A. N. Cleland, J. M. Martinis, and J. J. A. Baselmans, *Appl. Phys. Lett.* **99**, ArticleSequenceNumber:113507 (2011).
- [54] J. Kurkijärvi, *Phys. Rev. B* **6**, 832 (1972).
- [55] J. M. Martinis and H. Grabert, *Phys. Rev. B* **38**, 2371 (1988).
- [56] G. Oelsner, L. S. Revin, E. Il'ichev, A. L. Pankratov, H.-G. Meyer, L. Grönberg, J. Hassel, and L. S. Kuzmin, *Appl. Phys. Lett.* **103**, 10.1063/1.4824308 (2013).
- [57] P. Hänggi, P. Talkner, and M. Borkovec, *Rev. Mod. Phys.* **62**, 251 (1990).